Structural Studies of the Role of the Active Site Metal in Metalloenzymes

H. Feinberg, H. M. Greenblatt, and G. Shoham*

Department of Inorganic Chemistry and The Laboratory of Structural Chemistry and Biology, The Hebrew University of Jerusalem, Jerusalem 91904, Israel

Received September 22, 1992

This paper describes several experimental and computational methods which are currently used in the structural analysis of metal-containing macromolecules. A specific family of proteolytic enzymes which contain a zinc cation in the active site was selected to demonstrate these methods. A range of studies using one example from this family of enzymes is described which serves to clarify the role of the metal in the overall protein structure and in the local conformation of the active site in the native enzyme, the metal-deficient enzyme, and the metal-substituted enzyme and in complexes of the enzyme with various chemical analogues. The main experimental method described is X-ray crystallography, while computational methods for the examination of surface interactions and electrostatic potential effects are described briefly to complement the structural conclusions. The various experimental and computational results are then assembled in order to draw general conclusions on the structure–function relationships of metalloproteins and in particular the role of the metal in metal-containing proteolytic enzymes. The results of these studies implicate the zinc ion in the binding and catalytic activation of the substrate and stabilization of the tetrahedral reaction intermediate. It appears that in this family of enzymes a divalent metal cation is important for the required catalytic arrangement of functional groups in the active site, especially the metal ligands. However, once an appropriate metal ion is coordinated, there is practically no effect of the particular metal ion bound on either the overall three dimensional structure of the enzyme or the local detailed structure of its active site.

INTRODUCTION

The presence of various metal ions in proteins, and especially in enzymes has attracted the attention of both chemists and biochemists. The coexistence of metal reactivity in a protein environment makes the field of metallobiochemistry both interesting and important. Studies have shown that the biological role of a given metal depends not only on the specific protein and specific metal involved but also on the immediate environment of the metal within the protein and especially its coordination with the variety of protein ligands.

Among the transition metals the most common in proteins are iron and zinc.[1,2] While iron is located mainly in oxygen carrying proteins (e.g. myoglobin and hemoglobin) and oxidation/reduction proteins (e.g. ferredoxin and rubredoxin), zinc is located mainly in enzymes. Zinc is a good representative metal in the study of metallobiochemistry, since it is now known to be an essential component of more than 200 enzymes isolated from various species.[1-3] Although zinc can play either a catalytic, structural, or regulatory role, it is mainly found directly participating in catalysis.[1] Zinc-containing enzymes take part in biological reactions encompassing the synthesis and degradation of many major metabolites, and they are found in all six classes of enzymes. Especially well characterized is the class of hydrolases, and among those the most extensively studied is the family of zinc proteinases.[2,3]

The recent technological advancements in experimental and computational methods have merged with traditional biochemical methods to give powerful tools for the thorough study of metalloproteins. In the present paper we discuss the use of some of these approaches in a series of studies performed in our laboratory on the specific family of zinc proteinases. It should be noted, however, that although we focus specifically on zinc and zinc-containing enzymes, these studies may be performed (with minor changes) with other metal-containing proteins where the specific role of the metal in the biological activity is of interest.

ZINC PROTEINASES

Zinc-containing enzymes in which a divalent zinc ion is involved directly in the catalytic hydrolysis of peptide or protein substrates are categorized as a distinct family known informally as "zinc proteinases" (also "zinc proteases" and "metalloproteinases"). Unlike the families of serine proteinases, cysteine proteinases, and aspartic proteinases, where a relatively large number of enzyme and enzyme-complex structures are available, only a few high resolution structures have been reported for zinc proteinases. X-ray crystallographic investigations of four such enzymes are at various stages of completion. The four enzymes are: carboxypeptidase A (CPA),[4] carboxypeptidase B (CPB),[5] thermolysin (TLN),[6] and a D-alanyl-D-alanine cleaving carboxypeptidase, also called Zn-G peptidase or peptidase G (PEP-G).[7] While CPA and TLN have been extensively studied in the past decade, the other two (CPB and PEP-G) have been studied only to a limited degree. Recently, the structure of yet another zinc proteinase, neutral protease (NP), has been determined at 3-Å resolution.[8] This endopeptidase has been shown to be similar to TLN in both its sequence and structure.

Although TLN is not homologous to CPA (either in the amino acid sequence or in the overall structure), the catalytic site has been shown to be rather similar to that of CPA,[9-11] as demonstrated by the positions of specific functional groups relative to the catalytic zinc atom. From a comparison of the zinc environment of all these five enzymes, it becomes apparent that their active sites have a common three dimensional arrangement of catalytic residues, despite the fact that the proteins themselves have quite different folds. Because of the close similarity in the three dimensional structure of the active site of these five enzymes (and possibly also in other zinc proteinases), it is now believed that there is a common general mechanism behind the specific catalytic behavior of the different zinc proteinases,[12-14] in the same way that there is a common mechanism for the family of serine proteinases. In

0095-2338/93/1633-0501$04.00/0

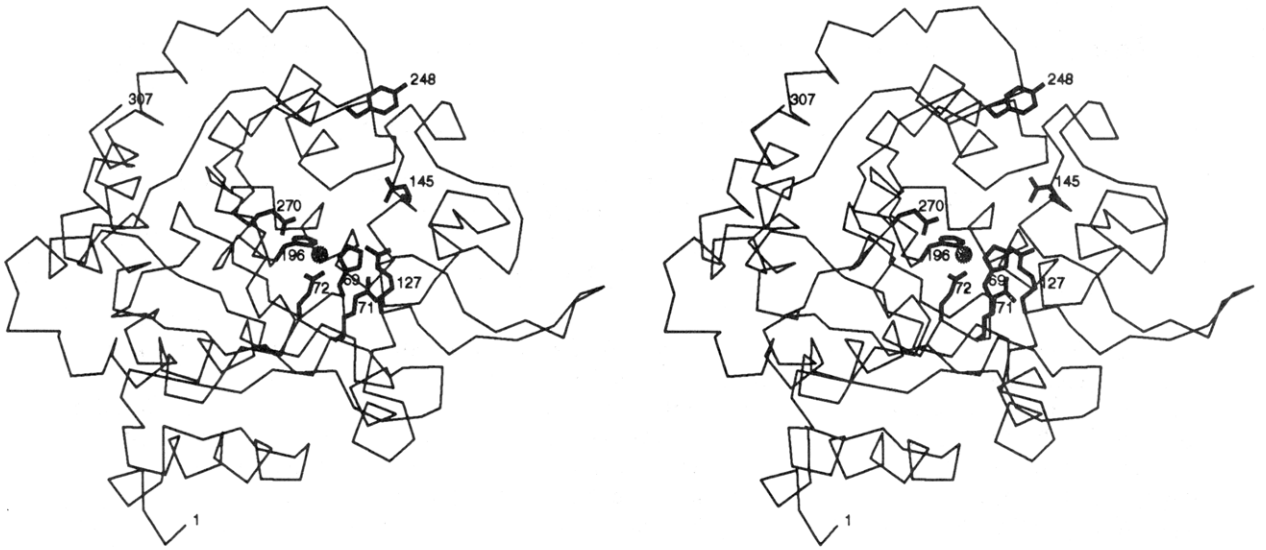

Figure 1. Stereo Cα representation of CPA, where the active site zinc is shown as a dot surface drawn at half its van der Waals' radius (center) and the side chains of key amino acid residues of the enzymatic reaction are shown.

order to determine this common mechanism, we performed a series of structural and kinetic studies on one of these enzymes, CPA, as a representative of the family of zinc proteinases. This enzyme was chosen primarily because it has been extensively studied in the past and since it forms stable crystals that diffract to high resolution.[14] It should be noted that with minor modifications these studies could be done on other zinc proteinases. In addition to providing a fundamental understanding of the zinc proteinases mechanism, the structure/function relationships in zinc proteinases are also important for practical purposes, since several zinc proteinases of yet unknown structure are involved in medically significant metabolic processes. The list of such enzymes include biologically important enzymes such as angiotensin converting enzyme (blood pressure regulation)[15] and enkephalinase (neuropeptide processing).[16]

CARBOXYPEPTIDASE *A*

The isolation,[17] characterization,[18,19] amino acid sequence,[20] and the three dimensional structure determination[4,21,22] of CPA are summarized in a number of reports and recent reviews.[1,2,13,14] The enzyme contains one zinc atom per molecule which is absolutely required for activity. CPA is a monomer and has a molecular weight of 34 000 (307 amino acids). Its crystal structure was first reported in 1968[21] and was subsequently refined at 1.5-Å resolution.[4] Its complexes with various inhibitors and analogues[23-34] and its structure at various pH conditions[35] are available from recent high resolution crystallographic studies. The Cα backbone trace of the high resolution structure of CPA is shown in Figure 1, where selected key active site amino acid residues are indicated.

CPA is often regarded as the prototypical zinc proteinase. It catalyzes the hydrolysis of the carboxy-terminus residue of peptides and carboxy-esters and exhibits specificity toward peptide or ester substrates bearing a large hydrophobic C-terminal residue such as phenylalanine. The zinc atom, situated in the active site, is pentacoordinated by two $N^{\delta 1}$ atoms of two histidine residues (His69, His196), the two O^{ϵ} atoms of a glutamic acid residue (Glu72), and one molecule of water. Reversible extraction of this metal atom creates an inactive enzyme,[18] while a replacement of it with a range of dications results in diverse activities[19] (Table I).

Bovine CPA readily gives large and stable crystals that diffract to high resolution. These crystals have one-third the

Table I. Peptidase and Esterase Activities of Metallo-CPA Derivatives[a]

	% activity			% activity	
derivative	peptidase	esterase	derivative	peptidase	esterase
apo	0	0	Hg(II)	0	116
Zn(II)	100	100	Pb(II)	0	52
Co(II)	160	95	Rh(II)	0	71
Ni(II)	106	87	VO(II)	23	50
Mn(II)	8	35	Cu(II)	0	0
Cd(II)	0	150	Co(III)	0	0

[a] Peptidase activity measured using N-CBZ-Gly-Phe (0.02 M), pH = 7.5. Esterase activity measured using HPLA (0.01 M), pH = 7.5.

peptidase activity of the dissolved CPA,[22] indicating structural similarity of the enzyme in the crystal and solution. Such similarity is also supported by other experimental and theoretical results.[13,35]

Extensive research related to CPA and its activity has been done in the past three decades,[2,14] and most of the functional groups essential for catalysis have been revealed. Nevertheless, the exact detailed mechanism of action of the enzyme has not been unambiguously determined, as discussed below. The important functional groups of the enzyme seem to be the carboxylic group of glutamate 270 (Glu270), the zinc atom, and possibly a zinc coordinated water molecule [$Zn(H_2O)$].[21] The role of the guanidinium group of Arg127 is not yet clear; however, recently it has been shown that this group may play an important role in both binding and catalysis.[25-29] Other amino acid residues indirectly participate in the catalytic activity of CPA, and they may possibly contribute to the binding of the substrate to the enzyme in the proper orientation. These are Arg71, Tyr198, Asn144, Arg145, Tyr248, and Phe279. In addition, Ser197 and Asp142 establish hydrogen bonds to active site functional groups[4] and might be directly (or indirectly) involved in either the binding or the catalysis. Kinetic experiments show that the substrate binding region extends to five amino acids of the substrate, and that the hydrolysis of longer substrates does not deviate significantly from Michaelis–Menten kinetics.[36]

POSSIBLE MECHANISMS

A number of mechanisms have been proposed for zinc proteinases, in general, and for CPA, in particular. These

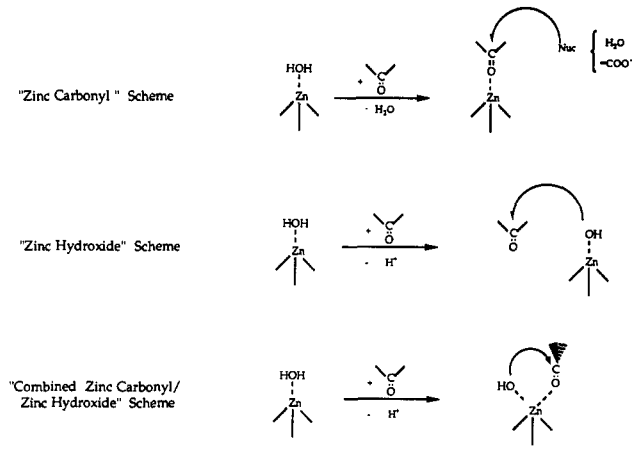

Figure 2. General schemes for three of the possible mechanisms for zinc proteinases.

mechanisms vary in the identity of activator, proton donor, and nucleophile.[4,13,14,21,37-39] The current discussion will focus on the initial stage of catalysis and especially on *the role of the metal* in the binding of the substrate, the promotion of the nucleophilic attack, and the stabilization of the resulting reaction intermediate. In this respect the initial stage of catalysis of the various possible mechanisms could be identified as one of three general categories: "*zinc carbonyl*", "*zinc hydroxide*", and "*combined*" mechanisms, simplified in the three schemes in Figure 2. These schemes demonstrate the differences in the possibilities of substrate/metal interactions and especially the roles of the zinc atom and the zinc-coordinated water in the catalytic pathway. In the zinc carbonyl scheme, the incoming substrate displaces the zinc-bound water and the carbonyl group of the terminal peptide bond of the substrate interacts directly with the zinc atom. In the zinc hydroxide scheme, the incoming substrate does not displace the zinc-bound water and the substrate carbonyl binds away from the zinc atom to allow a nucleophilic attack by the zinc-bound water. In the combined scheme, the incoming substrate does not displace the zinc-bound water; rather the substrate carbonyl interacts directly with the zinc atom via a pentacoordinated complex. The role of the zinc atom is hence significantly different in the three schemes. In the zinc carbonyl scheme, the zinc polarizes the carbonyl of the peptide bond, thus *activating the substrate* by making the carbonyl carbon more susceptible to nucleophilic attack. In the zinc hydroxide scheme, the zinc lowers the pK_a of the bound water, hence *activating the nucleophile*. In the combined scheme, the zinc interacts with the substrate as well as the nucleophile, hence *activating both the substrate and the nucleophile*.

The determination of the exact contribution of the metal in the overall catalytic pathway (polarizing electrophile, water promotion, etc.)[9,10,39] is of interest, of course, also for catalytic considerations of other metal-containing enzymes. As discussed above, the active sites in all of the zinc proteinases of known three dimensional structure display a similar arrangement of functional groups, including a negatively charged amino acid side chain ("base") and a positively charged amino acid side chain ("electrophile"), in addition to the zinc atom and its bound water molecule. These four elements are schematically arranged in two layers such that the upper layer of base/water/electrophile is approximately linear and located in a roughly symmetrical fashion above the zinc atom. This arrangement of the "catalytic tetrad" is schematically presented in Figure 3. Residues serving as the base could be glutamate or aspartate; those serving as the electrophile could be arginine, histidine, or lysine. The electrophile and its

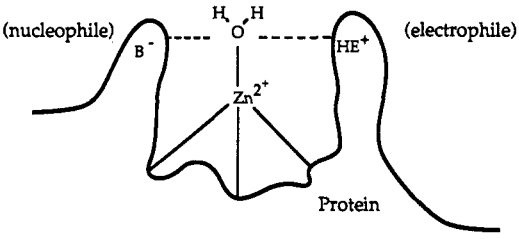

Figure 3. General geometry observed for the "catalytic tetrad" in zinc proteinases.

importance have only recently been suggested in view of the results of crystallographic studies of complexes of TLN[40] and CPA[25-29] and model building studies of TLN.[41] Thus, it appears that two additional residues join the zinc ion and the water molecule in the general catalytic mechanism of zinc proteinases, as proposed for both TLN[12] and CPA.[14] Exactly how such residues are involved in the proteolytic reaction and why their direct involvement is catalytically advantageous require further clarification.

UNRESOLVED QUESTIONS

Although the structure and activity of both CPA and TLN have been examined extensively via traditional kinetics and structural studies, the general mode of action of zinc proteinases is still not fully known. There are many unresolved questions which are related to the general mechanism of proteolysis of this family of enzymes. This is especially true of the binding and catalytic features which are common to all the members of the family. In this paper we would like to address only those specific questions which are directly related to the unique element of these enzymes, the active site zinc. We would like to examine the following points:

a. What is the effect of the metal on the overall structure of the enzyme and/or the fine structure of its active site?

b. What is the role of the metal in the binding mode and binding affinity of the enzyme toward substrates?

c. To what extent is the metal involved in activation of the substrate and/or the stabilization of catalytic intermediates?

d. What are the reasons for the dramatic changes in proteolytic activity of metal-substituted enzyme derivatives? Are these changes due to the changes in overall enzyme conformation, changes in active site structure, changes in substrate binding, or changes in the electrostatic/chemical nature of the specific substituted metal?

METHOD OF STUDY

In order to answer, at least in part, these and related questions, we have used in the past few years a combination of experimental and computational techniques: protein crystallography, enzyme kinetics, site specific mutations, surface interactions, electrostatic potentials, protein dynamics, and protein modeling. In the following discussion we describe the strategy, methodology, and results obtained from studies using crystallographic structural analysis combined with computational studies involving surface and electrostatic interactions.

The choice of crystallographic analysis for the structural studies is obvious since zinc is practically "transparent" to most spectroscopic methods. The general experimental strategy involves a series of high resolution structural studies of native (zinc) CPA, zinc-removed CPA, zinc-replaced CPA,

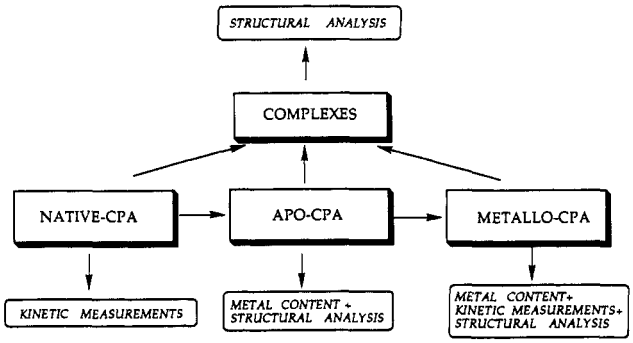

Figure 4. Experimental working scheme used for the study of structure–function relationships in CPA.

and complexes of these three classes of CPA derivatives with various nonproductive analogues, as schematically outlined in Figure 4. Analogues are molecules that closely resemble a catalytic species along the reaction coordinate and which cannot be cleaved by the enzyme due to a specific chemical difference from the corresponding "normal" (and productive) species. The need to study analogues rather than the actual substrates comes from the rather large difference in the time scale of the enzymatic reaction (milliseconds) and crystallographic data measurement (hours). Such "reaction coordinate analogues" could be molecules that closely resemble the substrate, the product, or any intermediate or transition state. These analogues are expected to interact with the enzyme in much the same way as a substrate or intermediate might, but are not labile to catalytic turnover, and thus remain bound in the active site of the enzyme. It is hoped that the integration of such reaction coordinate structures will lead-eventually to the elucidation of the complete mechanism of catalysis of zinc proteinases.

Since the three dimensional structure of native CPA is known to atomic resolution (1.5 Å)[4] and since most of the crystals of the metallo-derivatives and complexes of CPA that have been examined are isomorphous with the native crystals, one can take advantage of difference fourier synthesis techniques. This approach, when applicable, saves the need to determine the crystallographic phases of all measured reflections, a long and tedious process which is often the rate-limiting step in crystallographic analysis of macromolecules.

In general, in the case of small protein modifications (site specific mutations, metal replacement, etc.) as well as in the case of small inhibitors binding to large proteins, one can assume that the phase angle for each observed reflection from the modified protein/complex is nearly equal to the phase angle of each reflection from the native protein. The derived electron density, in theory, is completely featureless in those areas where the enzyme does not change as a result of the protein modification or the substrate/inhibitor binding. In areas where changes do take place, positions no longer occupied in the modified enzyme/complex that were occupied in the native enzyme give rise to negative electron density. Conversely, newly occupied regions that formerly did not contain atoms now show positive electron density. If the data are sufficiently good and extend to very high resolution (better than 2.0 Å), and the inhibitor binding or enzyme modification occurs with high statistical frequency, then the interpretation of the "difference" map is usually unambiguous and provides clear indications as to changes in the active site and the position of the inhibitor.

In the field of data collection, many recent advances in detection technology and analog–digital conversion have enormously improved data collection techniques. One of the most significant advances is the development of film replacement technologies in the form of imaging plate area detectors. An example of this new generation of detectors is the R-AXIS IIc (Rigaku Automated X-ray Imaging System) of Rigaku, Japan.[42,43] In this design, an europium-doped barium halide, ($BaFBr:Eu^{2+}$) is used to detect the diffraction. Impinging X-rays oxidize the europium to Eu^{3+} with the electron remaining trapped in the matrix, producing a "color-center" (or "F-center"). Scanning the plate with 633-nm laser light causes fluorescence at these color-centers at 400 nm, which is detected by a photomultiplier tube. The amount of fluorescence is proportional to the intensity of the impinging X-rays at a particular position of the imaging plate. Thus, the scan of the plate results directly in a two dimensional digitized image of the diffracted ("raw") data. The plate is then erased by a short exposure to high intensity light, in order to completely remove all "color-centers", resulting in a blank plate which is now ready for further use. The re-use of the imaging plate not only provides an economical and efficient means for diffraction measurement but also allows for a fully automated data collection. Although this technology has been introduced to crystallography only recently, its advantages are clear and thus expected to be the future standard technology in macromolecular crystallography.[43,44]

Once a model is fit to the electron density map by hand (using three dimensional graphic display workstations), mathematical refinement programs are used to improve the model relative to the observed diffraction data. Restraints are usually placed on the atomic positions, based on values of ideal bond lengths, bond angles, and planarity, obtained from small molecule crystal structures. For starting or incomplete models, loose restraints are used. These are gradually tightened as the refinement progresses and the quality of the model is improved. One of the most widely used methods of restrained least-squares refinement is the algorithm developed by Hendrickson and Konnert.[45] It is sometimes useful to add various degrees of energy minimization to the refinement procedure, so that the resulting molecular model will not only agree with the observed data and ideal molecular geometries but will also have an optimized overall energy.[46]

In any procedure of refinement one ends up with a final molecular model whose reliability depends mainly on the amount of diffraction data measured and the agreement between observed and calculated diffraction intensities. The amount of data is proportional to the maximal diffraction angle measured ($2\theta_{max}$) and is related to the minimal interlayer spacing (d_{min} by Bragg's law ($d_{min} = \lambda/(2 \sin \theta_{max})$). The value d_{min} is given in angstroms and is commonly called the *resolution* of the data observed and/or collected. The higher the observed θ_{max} (the lower d_{min}), the higher the resolution and the better defined the resulting structure. The agreement between observed and calculated data (F_o's and F_c's, respectively) is reflected in the commonly used crystallographic *R-factor* ($R = (\sum|F_o - F_c|)/\sum F_o$, where the summation is over all measured reflections). In this case a lower R-factor signifies better agreement between the observed and calculated data. For the following discussion it is important to note that as d_{min} decreases (higher resolution) and the R-factor decreases (better agreement), the final structure is more reliable. An analysis of the R-factor as a function of the errors in atomic positions alone has been carried out by Luzzati[47] in order to provide an upper limit to the expected error (Δr) in the atomic positions at particular values of R and resolution. It has been shown that for a refined structure with $d_{min} = 1.5$ Å and $R = 15\%$ the typical Δr in the atomic coordinates is around 0.1 Å, while

Table II. Data Collection and Refinement Parameters for the Newly Refined Structures of Native-CPA (**) and Apo-CPA (***) Compared with the Corresponding Parameters of the Previously Published Structure of Native-CPA (*)

	native-CPA*	native-CPA**	apo-CPA***
no. of crystals	3	1	1
resolution (Å)	1.54	1.48	1.90
no. of unique reflecns	32 080	34 352	21 540
R_{sym}/R_{merge}	0.10	0.04	0.08
no. of refinement cycles	51	36	32
no. of water molecules	192	217	199
rms deviation (σ, target)			
bond lengths	0.024 (0.017)	0.017 (0.015)	0.013 (0.015)
av ω (deg)	8.5 (6.4)	2.8 (2.5)	2.3 (2.5)
final R-factor	0.190	0.148	0.159

for a similar structure with d_{min} = 2.0 Å and R = 20% the typical Δr is around 0.2 Å. Since most of the structures presented in the following have been refined to final R-factors of 15–18%, for data of 1.5–1.8-Å resolution, the upper limit for the typical error in coordinates and interatomic distances in these structures is in the range of 0.1–0.2 Å. Such estimates of structural errors are extremely important for critical evaluation of small conformational changes in a series of slightly different macromolecular structures. The question of the significance of structural differences is especially important if the structural results provide the basis for conclusions involving detailed mechanisms of action or detailed modes of binding.

HIGH RESOLUTION STRUCTURES OF NATIVE- AND APO-CPA

Although the structure of native carboxypeptidase A (native-CPA) has been solved to high resolution,[4] the diffraction data used in the refinement of the structure were a compilation of single counter diffractometer data sets which were measured on several crystals and gathered over several years of study. In addition, it was found recently from a bovine cDNA sequence of CPA[48] that there are seven misassignments of amino acid side chains (Asp/Asn and Glu/Gln) in the originally determined polypeptide sequence. These misassignments are not uncommon in amino acid sequences determined by protein sequencing, and in the case of CPA they do not involve critical catalytic amino acid residues. Nevertheless, in the process of refinement of a structure at atomic resolution such small sequence corrections may be of significance in the interpretation of hydrogen bond configurations.

Our initial goal in the structure/activity study was to obtain the best possible high resolution structure of native-CPA, based on higher quality area detector diffraction data from a single crystal and refined with the corrected sequence. This was done to provide the highest quality structure possible for use as a reference for zinc replacement studies and inhibitor–binding studies, since the changes in the atomic positions for these derivatives may be small.

Data from a crystal of native-CPA were collected to 1.48-Å resolution on an R-AXIS IIc, with a graphite monochromator, as summarized in Table II. The enzyme structure was then refined using a restrained least-squares method.[45] The results of the refinement are summarized in Table II. The improvement in the quality of the model is apparent from the comparison of the R-factors and geometry parameters between the older model of CPA and this newer one. In general, tighter geometry and lower R-factor are indicative of a more accurate model. The number of water molecules identified in the final structure was also subject to stringent criteria, where residual peaks in the electron density map were not assigned as water molecules unless the height of the peak was at least three times that of the root-mean-square (rms) deviation of the map and occupied more than one grid point in space.

In order to clarify what role the metal ion might play in both the maintenance of the structure of CPA and in its mechanism of action, the metal ion was extracted from crystals of CPA, yielding apo-CPA. Atomic absorption measurements showed that virtually all the zinc (>99%) had been extracted from the crystals. The crystals of apo-CPA were then subjected to a full structural analysis. Diffraction data were collected to high resolution (1.9 Å) and refined to a final R-factor of 15.9%. As can be seen from Table II, the quality of this structure is comparable to the quality of the model for the native enzyme, and thus meaningful conclusions can be drawn from even small (~0.2-Å) changes in the structure.

In general, the structure of apo-CPA is very similar to the native enzyme as reported in earlier lower resolution studies.[24] As demonstrated in Figure 5, the only major change which took place upon removal of the zinc is that one of the zinc ligands, His196, rotated 110° about χ^2, to form a salt bridge with Glu270, indicating that the zinc atom does not play a very large role in maintaining the overall native conformation of the enzyme.

A partial conclusion of this portion of the study, then, is that the zinc atom does not play a role in maintaining the conformation of the active site of CPA as a whole, and that the loss of activity observed upon removal of the zinc ion is due to the absence of the metal alone, and not because of large structural changes.

Attempts were then made to obtain complexes of apo-CPA with inhibitors and analogues in order to examine what role the zinc ion may play in binding substrates. In addition, it was hoped that information about the possible roles of other active site functional groups in binding might be revealed. Moreover, the structure of the apo-enzyme with an inhibitor, or a substrate, might give a model for the Michaelis–Menten (precatalytic) complex. The structure of the Michaelis–Menten complex is especially relevant in determining whether or not different types of substrates have different initial binding modes. High resolution data sets were collected on a series of crystals of the apo-enzyme which had been soaked with several high affinity substrates and inhibitors (ketomethylene and benzyl succinate derivatives). These structures were then refined to convergence (with final R-factors of less then 17%). It was interesting to find that in this series of refined structures (of potential apo-CPA complexes) none of the inhibitors nor any of the peptide substrates were seen bound in the active site. These negative binding results indicate that, for these types of peptide substrates and inhibitors, the zinc ion plays a direct and significant role in binding. The results for the peptide substrates seem contrary to the hypothesis that initial complex formation between CPA and peptide substrates does not involve the zinc atom.[14]

METALLO DERIVATIVES OF CPA

As discussed above, the zinc ion in CPA may be freely removed, with concomitant loss of activity; readdition of zinc restores full activity. An enzyme with a different active site metal can also be obtained by the replacement of zinc with other transition metals. Activity of metal-substituted CPA toward a peptide and an ester is shown in Table I above. A loss of activity could be caused by several factors, such as a change in active site conformation, a change in the metal ligand conformation, or a change in the binding mode of

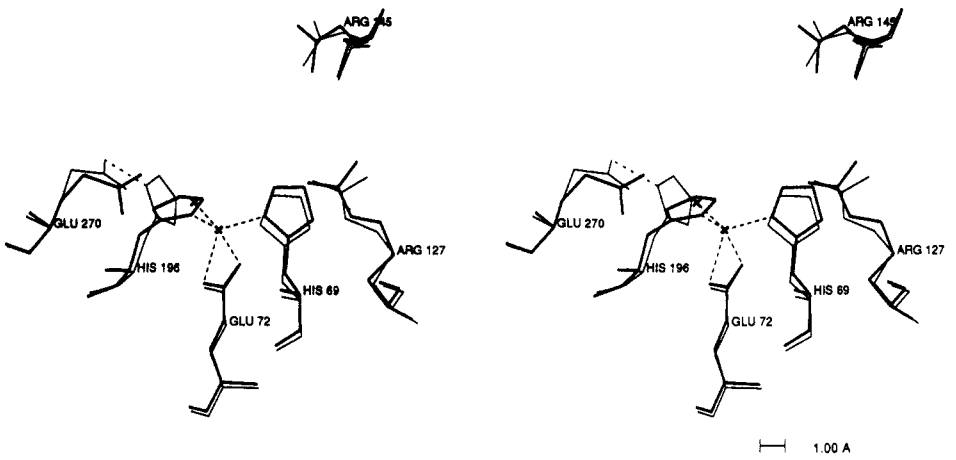

Figure 5. Stereoview comparison of the active site of native-CPA (thick lines) and apo-CPA (thin lines), showing that there is little overall change in the conformation of the side chains of the residues that are in the vicinity of the zinc. The major exceptions are His196 and Glu270 which now form a salt bridge (distance shown is 2.9 Å).

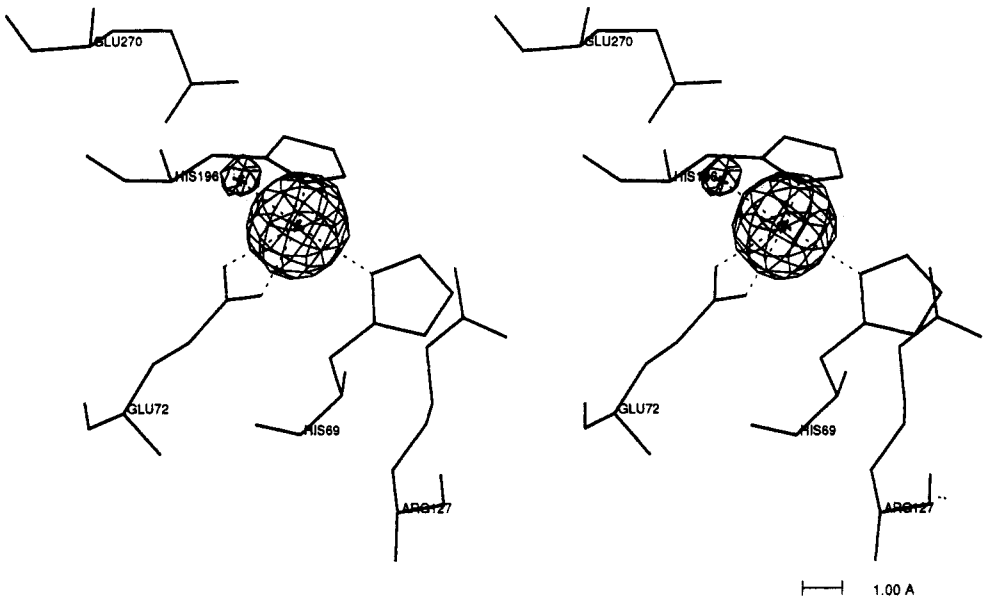

Figure 6. Difference fourier ("omit") map of the active site of Cd-CPA (stereoview). The map was calculated with $F_o - F_c$ fourier coefficients. For this calculation, the final model of Cd-CPA was used, but with the Cd atom and its water molecule removed. Contouring of the electron density is done at 3σ, where σ is the root-mean-square (rms) deviation of the electron density map.

substrates. Alternatively, different metals have different electronic properties and, as a result, change the kinetic parameters of the reaction. In order to investigate the former possibilities, we prepared several metal derivatives of CPA by soaking crystals of the apo-enzyme with the corresponding chloride salts of the desired metal.[49] Special care was taken to avoid traces of undesired metals (particularly zinc) in all the solutions involved in the metal exchange procedure. In all cases it has been confirmed by atomic absorption that at least 98% of the active site zinc has been replaced with the metal ion of interest.

Crystals of the metallo derivatives of CPA were then subjected to detailed crystallographic analysis at the highest resolution available, and the resulting structures were compared to the native enzyme and to each other. Of these metallo-CPA structures we present here only those of Mn-CPA, Cd-CPA and Hg-CPA, for which atomic resolution data have been measured (1.82, 1.82, and 1.76 Å, respectively) and refinement converged to low R-factors (17.4, 16.3, and 14.8%, respectively). Since all three structures were found to be highly isomorphous with the native enzyme, it was possible to examine the details of the metal environment directly from the electron density difference maps.

An example of this type of map is shown in Figure 6 where the active site of Cd-CPA is presented together with a Fourier difference map. The electron densities for Cd and the Cd-bound water are clearly observed, and their positions can be accurately located. Although the movement of active site residues can be deduced from the positions of the relevant positive and negative electron densities in the difference map, a clearer picture of the active site was obtained by calculating a difference map against a native enzyme model in which the active site residues had been removed. The resulting electron densities were clearly interpretable and used to rebuild all those amino acid residues for which slight conformational changes are observed in the initial difference map. Figure 7 shows a rebuilt and refined model of the active site of Cd-CPA superimposed on the corresponding region of native-CPA (Zn-CPA). In this figure it is demonstrated that the enzyme active site and even the first coordination sphere of the metal have not been changed significantly by the metal replacement. The only obvious change observed between the two structures is the exact position of the metal-bound water. While in the native enzyme this water is located in the geometrically apical position, in the Cd enzyme, the water molecule seems to be asymmetrically located, such that it is

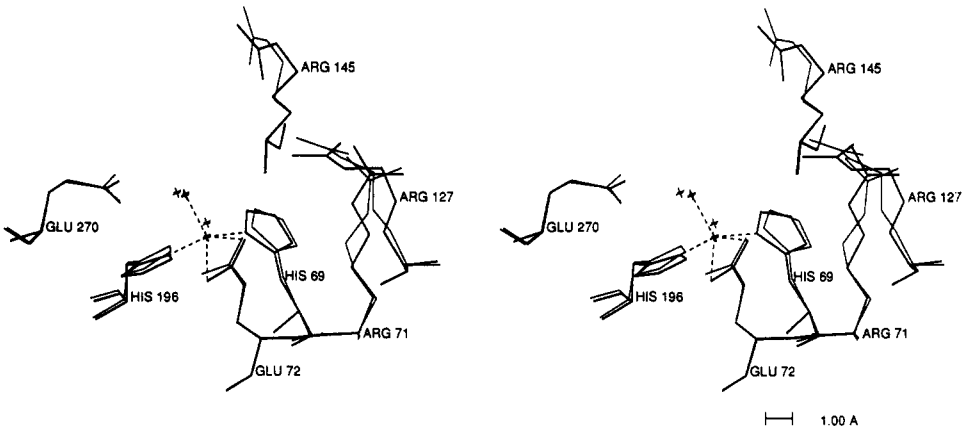

Figure 7. Stereoview comparison of the active sites of native-CPA (thick lines) and Cd-CPA (thin lines), showing that replacement of the metal does not bring about major changes in the conformations of key active site residues.

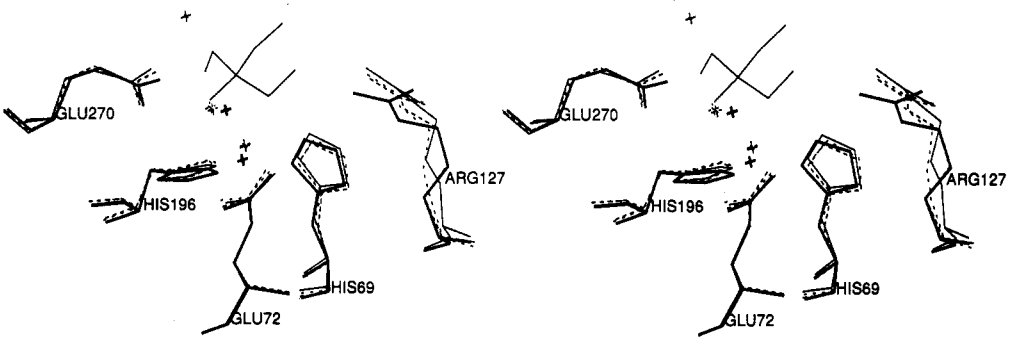

Figure 8. Detailed stereoview of the active sites of native-CPA (thick lines), Hg-CPA (thin lines), Mn-CPA (dashed lines), and Cd-CPA (dotted lines). Also included are the additional features observed in two of the Hg-CPA structures: a Tris solvent molecule taking the place of a water molecule and the extra cation bound to Glu270 (see text).

Table III. Metal–Ligand Interactions (Å) in CPA Derivatives

derivative	Zn-CPA	Mn-CPA	Cd-CPA	Hg-CPA
M–His69	2.00	2.34	2.37	2.26
M–His196	2.08	2.32	2.13	2.22
M–Glu72	2.30	2.12	2.17	2.57
	2.32	2.57	2.43	2.68
M–water	1.95	2.17	2.39	2.41
Glu270–water	2.63	2.70	2.50	
	3.34	2.71	2.63	
Arg127–water	4.65	6.06	6.28	

closer to Glu270 and further removed from Arg127. Nevertheless, aside from the water position and small conformational deviations, the two active sites are practically identical.

Similar structural analysis has been carried out with Mn-CPA and Hg-CPA. The refined structures of the three metallo derivatives were then superimposed on each other and compared with the native enzyme. As demonstrated with Cd-CPA no significant differences were found in the overall structure of the enzyme and only slight changes were observed in the metal–protein or metal–water interactions. These results correlate well with previous structural reports concerning zinc-substituted derivatives of CPA.[50,51] The structures of Zn-CPA, Mn-CPA, Cd-CPA, and Hg-CPA are compared in Figure 8, and the corresponding metal–ligand distances are given in Table III. As expected from the differences in the ionic radii of the metals involved, the metal–ligand distances generally increase with the ionic radii expected (Hg being the largest of this series), yet the interligand angles and the metal coordination geometry remain very similar. As noted above for Cd-CPA the metal-bound water in all three derivatives moves toward Glu270 (the assigned "base" of the catalytic tetrad) relative to the native enzyme, forming hydrogen bonds with both carboxylic oxygens of its side chain. It could be claimed that such stronger interaction of the metal-bound water with an enzyme residue makes it more difficult to be removed by the incoming substrate and thus accounts, at least in part, for the reduced activity of these derivatives. Nevertheless, the differences in water position are relatively small and are not likely to contribute, for the most part, to dramatic changes in activity. Since for practical considerations there is no significant change apparent in the structures of these metal derivatives, the possibility that changes in metal binding or in the metal environment are responsible for the observed difference in activities becomes less likely.

It is important to note that the correlation of activity and structure by comparison of related structures requires special attention to the experimental conditions. For example, in one of the Hg-CPA structures studied, where the crystallization solution contained Tris buffer (Tris = 2-amino-2-(hydroxymethyl)-1,3-propanediol), the final model indicated the presence of a Tris buffer molecule in the active site, as suggested earlier by Rees *et al.*[51] This buffer molecule was acting as a ligand to the mercury ion via its amino group, an interaction that is expected from the high affinity of mercury to nitrogen ligands. In addition to this unexpected result, another structure of Hg-CPA, where the crystals had been soaked in a solution of inhibitor, showed an additional cation (with scattering characteristics of Ca or first row transition metals) bound to Glu270. These observations suggest that in certain experimental conditions some of the observed losses of activity for various metals may be artifacts, caused by competitive inhibition of impurities or solvent/buffer molecules. For the structural comparison with the other metal derivatives we used the Hg-CPA/Tris structure rather than the Hg-CPA one since it was of higher quality and resolution. The two Hg-CPA structures were otherwise identical.

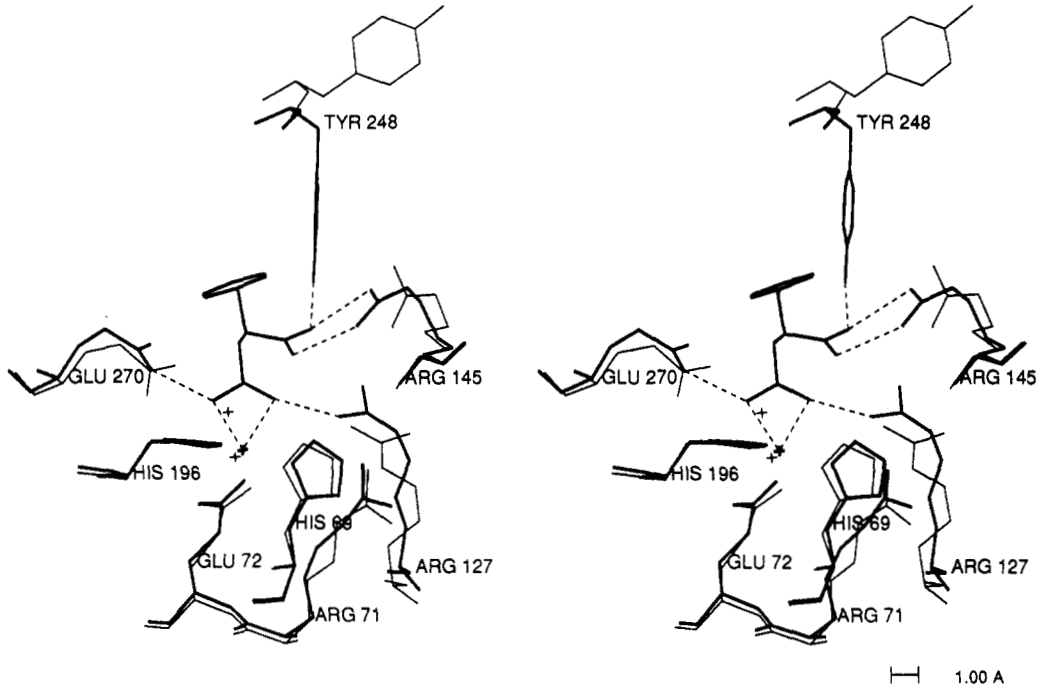

Figure 9. Stereoview of the active site of native-CPA (thin lines) vs benzyl succinate/CPA complex (thick lines). Dotted lines represent interactions in the complex.

COMPLEXES OF METALLO-CPA WITH INHIBITORS

In order to address the possibility that metal substitution causes a change in substrate binding rather than a change in the active site, we crystallized complexes of specific high affinity analogues with native CPA and a series of metallo-CPA derivatives. Here we present the structural results obtained from the complexes of a particular inhibitor, benzyl succinate (BS), with native-CPA (Zn-CPA) and two metal substituted derivatives, Hg-CPA and Ni-CPA. BS was the first affector chosen for this purpose since it binds strongly to CPA,[52,53] and it has been the target model of much effort in drug design for zinc proteinases.[54,55] In fact, BS represents a family of dicarboxylate anions, all of which are competitive inhibitors of CPA.[52,56] Among those compounds BS is the most potent inhibitor for both peptide and ester hydrolysis ($K_i = 4.5 \times 10^{-7}$ M).[53] The high affinity of BS to CPA has been explained by its resemblance to the collected products of peptide hydrolysis and was therefore considered originally as a "biproduct analogue". It contains a moiety analogous to the terminal amino acid (L-phenylalanine) which is cleaved, and an additional carboxylate group that mimics the carboxy-terminus carboxylate of the newly formed peptide.

The complex of native-CPA with BS and the corresponding complexes of Ni-CPA/BS and Hg-CPA/BS have been prepared by the soaking of the corresponding CPA crystals with BS solution. In all three cases BS was found in the active site at close to full occupancy, while the crystals remained isomorphous and diffracted to high resolution. Experimental conditions for all three complexes were kept similar in order to minimize solution effects and isolate only metal effects in the binding of the inhibitor. Crystallographic diffraction data sets for the complexes of Zn-CPA/BS, Ni-CPA/BS, and Hg-CPA/BS were collected and refined to final *R*-factors of 15.0% (at 1.7-Å resolution), 15.8% (at 1.7-Å resolution), and 14.5% (at 1.8-Å resolution), respectively. In all cases the initial difference map showed complete electron densities for the bound BS molecule and indicated clearly the resulting conformational changes in the active site. The detailed binding of BS to the active site of native-CPA is shown in Figure 9, where it is superimposed on the corresponding region of the unbound native enzyme. As demonstrated in this superposition, the BS molecule displaces the metal-bound water and binds in the general position usually occupied by bound analogues and inhibitors[14,29] while causing the commonly observed conformational changes in the active site. The main features of this structure correlate with a recently published lower resolution structure of CPA/BS,[32] although some structural details are different in the two structures and may be due to the resolution limits involved. The terminal carboxylate (C-carboxylate) forms a salt bridge with the guanidinium group of Arg145 and hydrogen bonds with Tyr248 and Asn144. Tyr248, as expected, is rotated into the "down" position allowing better interactions with the bound inhibitor and blocking off the active site from solvent. This large conformational change of Tyr248 is linked to a distinct conformational change of the peptide chain in the region of residues 246–250, which is beyond the scope of the present discussion.

Of main interest is the second BS carboxylate group (A-carboxylate) which is bound to the zinc ion as a nearly symmetrical bidentate ligand, replacing the water molecule of the native structure in the apical ligand position. This result is energetically reasonable, yet it was not expected since in the analogous complex of BS with TLN the A-carboxylate of the inhibitor is bound to the metal as a monodentate ligand.[57] In the present CPA/BS complex, the zinc ion moves about 0.4 Å from its original position toward the bound inhibitor. One should note that in addition to the metal binding the A-carboxylate forms close contacts with both *Glu270* (the tetrad "base") and *Arg127* (the tetrad "electrophile"). The two critical catalytic functional groups are positioned symmetrically on the two sides of the carboxylate group, where $N^{\eta 1}$ of Arg127 is 2.6 Å from one of the carboxylate oxygens (O1) and $O^{\epsilon 1}$ of Glu270 is 2.6 Å from the other carboxylate oxygen (O2). Note that this implies the existence of a hydrogen between the inhibitor carboxylate (O2) and Glu270. These strong hydrogen bonds contribute further stability to

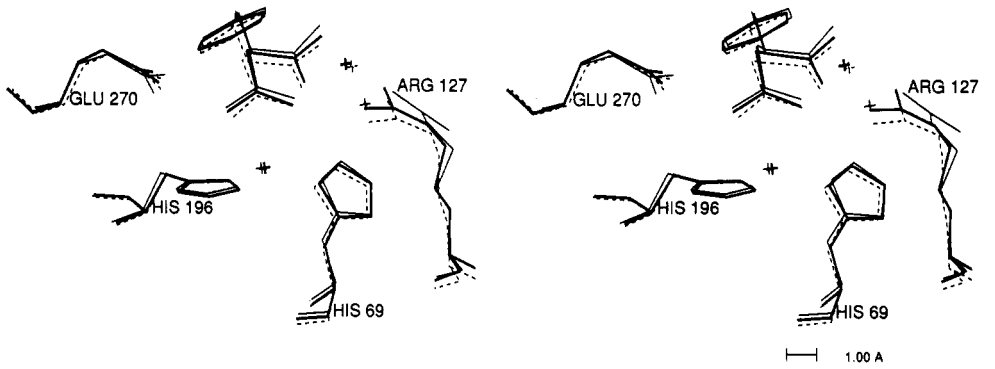

Figure 10. Stereoview comparison of three benzyl succinate complexes: native-CPA (thick lines), Hg-CPA (thin lines), and Ni-CPA (dashed lines). Note the difference in the conformation of Arg127 in Hg-CPA, with the addition of a water molecule between the side chain and the inhibitor.

Table IV. Active Site Interactions (Å) in CPA/BS Complexes

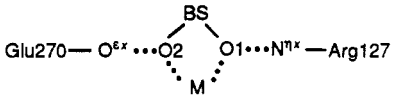

complex	Glu270–$O^{\epsilon x}$–O2	M–O2	M–O1	Arg127–$N^{\eta x}$–O1
Zn-CPA/BS	2.61 ($O^{\epsilon 1}$)	2.30	2.36	2.61 ($N^{\eta 1}$)
	3.41 ($O^{\epsilon 2}$)			3.47 ($N^{\eta 2}$)
Ni-CPA/BS	2.72 ($O^{\epsilon 1}$)	2.35	2.22	2.77 ($N^{\eta 1}$)
	3.52 ($O^{\epsilon 2}$)			3.46 ($N^{\eta 2}$)
Hg-CPA/BS	2.73 ($O^{\epsilon 1}$)	2.43	2.64	3.59 ($N^{\eta 1}$)
	2.65 ($O^{\epsilon 2}$)			

the enzyme–inhibitor complex. Such strong interactions between the A-carboxylate and the base/electrophile functional groups of the active site, and the combination of these interactions with the strong bidentate interactions with the metal, may account for the strong inhibitory properties of BS. These types of interactions are likely to be relevant also for other carboxylate inhibitors and analogues and hence may be of general importance.

Similar structural analysis has been performed with the BS complexes of the other metallo-CPA derivatives. The final structures of Zn-CPA/BS, Ni-CPA/BS, and Hg-CPA/BS are compared in Figure 10, where the metal coordination environments in the three structures are superimposed. The actual distances between the main functional groups of the three structures are listed in Table IV. As can be seen from these structures, in general there are no significant changes in the binding geometry of BS when the active site metal is changed. A noticeable difference is observed in the case of Arg127 in the mercury derivative. In this structure, the side chain of Arg127 appears to adopt a conformation similar to that found in the native (unbound) structure. In this structure the interaction of the inhibitor carboxylate oxygen with Arg127 $N^{\eta 1}$ is replaced by a hydrogen bond to a water molecule (2.6 Å), which in turn hydrogen bonds to the N^{ϵ} (2.2 Å) and $N^{\eta 1}$ (2.2 Å) of Arg127. Nevertheless, although there are some small structural differences in the three active sites, in general the bound inhibitor binds in the same location and forms similar interactions with active site residues. Most importantly, the three metals bind the A-carboxylate of the inhibitor in much the same bidentate fashion. Even the metal carboxylate distances are comparable, if one considers the differences in ionic radii of the three metals involved. It is concluded, therefore, that the general mode of binding of BS is not affected by the specific metal present in the active site. Since BS resembles a whole family of inhibitors and analogues, these results suggest that the mode of binding may not be metal dependent for substrates as well, and hence the differences in observed activities of various metallo-CPA derivatives are not likely due to differences in substrate binding.

COMPLEXES OF NATIVE-CPA WITH TRANSITION-STATE ANALOGUES

Another method for studying the early stages of enzymatic mechanisms is to examine the complexes of the enzyme with nonreactive analogues resembling substrates. The complexes of CPA that have been examined to date are those with GlyTyr,[21,24] an inhibitor from potatoes,[23] and several amino acids, aldehyde, ketone, phosphonate, and phosphonamidate analogues.[25-28,30-34] Interesting structural changes occur to CPA residues in the active site upon contact with these analogues and inhibitors, from which the main features of substrate interactions with the enzyme have been deduced. A considerable drawback in these studies is the fact that all these substrate-like molecules seem to behave abnormally, deviating from Michaelis–Menten kinetics or from normal catalysis in general.

For these reasons we designed a new series of substrate analogues to be used in crystal structure analysis. This is the series of di-, tri-, and tetrapeptides containing one pseudopeptide bond strategically placed at the carboxy terminus.[58] This peptide bond is replaced with a ketomethylene bond, i.e. $-CH_2-$ is substituted for –NH–. The advantage of these analogues over those previously used compounds is their similarity to natural peptides, both in residue types and in peptide conformation. Furthermore, these analogues are resistant to cleavage in the active site of CPA due to the strength of the CO–C bond versus the CO–N peptide bond. These analogues have the general structure X-(*R*,*S*)Phe-Ψ(CO–CH_2)-(*R*,*S*)-Phe-OH (Ψ represents a ketomethylene bond [–$COCH_2$–] rather than the normal peptide bond [–CONH–]), where X is a moiety with varying size and hydrophobicity.

Several such analogues (Ac-PheΨPheOH, I; pGlu-PheΨPheOH, II; Boc-PheΨPheOH, III; Bz-PheΨPheOH, IV; Boc-Phe-PheΨPheOH, V; NH_2-Ala-PheΨPheOH, VI) were prepared, mimicking the blocked dipeptide PhePheOH, the blocked tripeptide PhePhePheOH, and the unblocked tripeptide AlaPhePheOH, all of which are good natural substrates for CPA. These pseudopeptides were examined kinetically, and were found to bind to the enzyme with high affinity and exhibit considerable competitive inhibition (K_i's in the submicromolar range).[59,60] The specific K_i's observed seem to be significantly dependent on the size and hydrophobicity of the blocking group (X), a fact that is very important for the design of second generation inhibitors. Analogues I–VI were then reacted with native CPA, and the resulting complexes were crystallized. In the following we discuss the structures of the

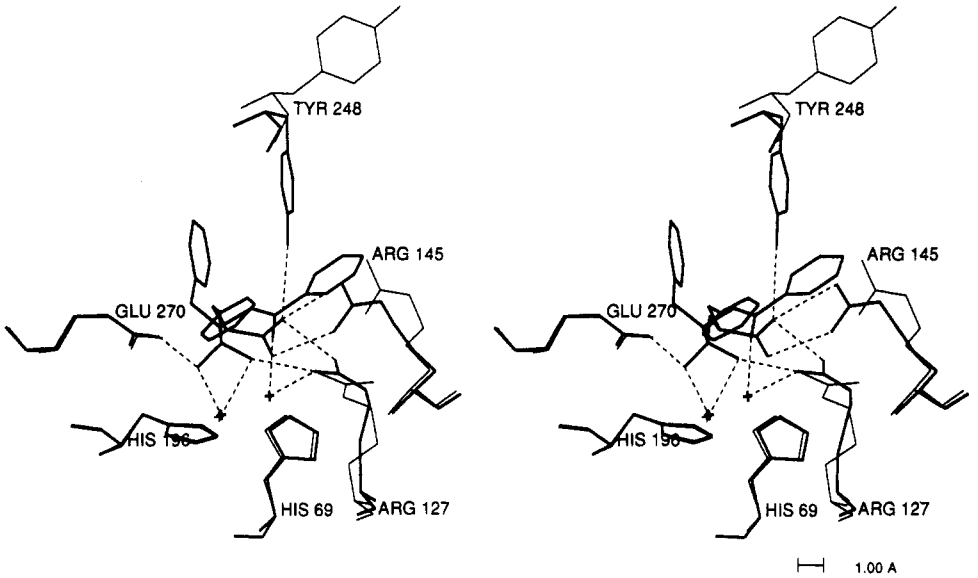

Figure 11. Stereoview of the active site of CPA showing binding of benzoyl-Phe-Ψ-Phe to CPA (thick lines) relative to native-CPA (thin lines). Dashed lines represent hydrogen bonds or other favorable electrostatic interactions.

CPA complexes of I, III, and IV, for which the crystals were found to be isomorphous to the crystals of native-CPA and for which high resolution data were collected. The structures of CPA/I, CPA/III, and CPA/IV have been refined at high resolution, and converged to final *R*-factors of 14.8% (at 1.7-Å resolution), 23.6% (at 1.75-Å resolution), and 15.5% (at 1.7-Å resolution), respectively. A more detailed structural discussion of the CPA/III complex has been presented elsewhere.[29] In all three cases the initial difference map indicated the binding of the analogue in the active site and apparent removal of the zinc-bound water. In all cases the analogue is directly interacting with the zinc and causes the typical conformational changes in the active site of the enzyme. In fact, since the analogue is bound statistically to only a fraction of the enzyme molecules in the crystal (with total occupancy of 0.5–0.8), it is possible to compare the conformations of the active site residues before and after the binding. For example, in the crystals of the CPA/IV complex about half of the CPA molecules have bound analogue while the other half of the molecules have no analogue bound. Due to the quality and resolution of the diffraction data, it was possible to resolve the two conformations involved and hence to determine and refine in parallel the structures of the complexed and uncomplexed native enzyme within the same crystal. The two conformations are shown in Figure 11, where a classical case of "induced fit" of an enzyme is presented. Most of the conformational changes observed upon binding of the ketomethylene analogue are those typically observed with bound affectors and have been discussed in detail before.[14,29] It is interesting to note that most of the active site residues, including the three arginines (71, 127, and 145), Tyr248, and Glu270, have moved noticeably from their positions in the native enzyme to accommodate the binding of the analogue.

The region of interest, however, is the zinc environment and the metal–analogue interactions. The electron density difference map around the ketomethylene bond shows well-defined bifurcated electron density corresponding to a *hydrated ketone*. That is, the species observed bound to the enzyme is the tetrahedral hydrated form of the original carbonyl, similar to the proposed tetrahedral intermediate formed during the cleavage of substrate. This was initially a surprise since this particular ketone does not posses an exceptionally electrophilic carbonyl, and therefore is not expected to exist in aqueous solution in a hydrated form.[29] Hence, this enzyme/inhibitor complex is a stable species resembling *a structure along the reaction coordinate* of this chemical reaction, rather than a species resembling a reactant or a product. The results obtained from this pseudopeptide, as well as the other ketomethylene pseudopeptides, strongly support the supposition that after the initial binding to the enzyme the ketonic carbonyl is attacked by a water molecule (presumably the zinc-bound water) resulting in a stable *gem* diol. Since the scissile peptide bond has been replaced by a less reactive one, cleavage cannot take place, and the inhibitor remains tightly bound to the enzyme. The hydrate formed directly interacts with the zinc ion as a bidentate ligand, replacing the zinc bound water in the native enzyme. The two hydrate oxygens are arranged above the zinc ion with typical zinc–oxygen distances of 2.2 and 2.6 Å. Interestingly, the *gem* diolate is further stabilized by close interactions with the two other active site residues. One hydrate oxygen (O1) receives a hydrogen bond from Arg127, and the other hydrate oxygen (O2) forms a hydrogen bond to Glu270.

A similar arrangement of the *gem* diol, the zinc ion, and the active site catalytic residues is observed in the refined structures of the complexes of CPA with analogues I and III. The three structures are compared in Figure 12, and the relevant bond distances are listed in Table V. In all three cases the resulting *gem* diolate interacts closely with the zinc ion and also with Arg127 and Glu270. In fact, in the cases of analogues I and IV two such interactions are present between each of these residues and the corresponding hydrate oxygens (Table V). Such strong interactions account, at least in part, for the strong binding of these inhibitors, and if we consider them as reaction intermediate analogues, these interactions suggest the possible role of the zinc ion and the catalytic residues in the stabilization of a true catalytic intermediate of the enzymatic hydrolysis.

Aside from providing a model of the tetrahedral intermediate, the detailed structure of the complexes of the ketomethylene analogues with CPA also give insights into how different blocking groups interact with the extended active site of the enzyme. Since these analogues are also potent and selective inhibitors, this information is useful for drug design. Although not discussed above, the analogue–enzyme interactions observed in the outer binding cleft (where the X

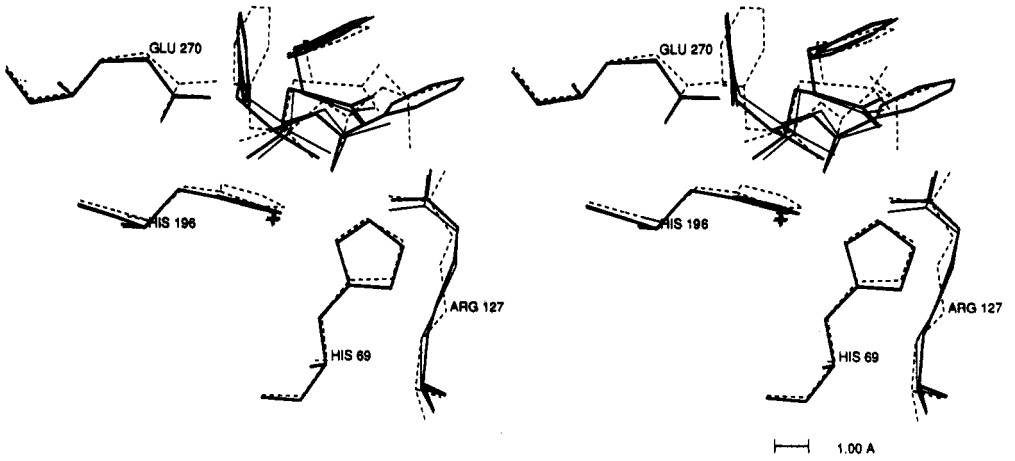

Figure 12. Stereoview comparison of three ketomethylene inhibitors bound to CPA: benzoyl-Phe-Ψ-Phe (IV, thick lines), acetyl-Phe-Ψ-Phe (I, thin lines), and BOC-Phe-Ψ-Phe (III, dashed lines).

Table V. Active Site Interactions (Å) in CPA/KM Complexes

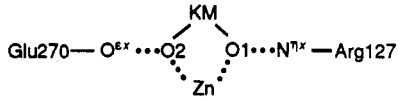

complex	Glu270–O2	Zn–O2	Zn–O1	Arg127–O1
Zn-CPA/I	2.69 ($O^{\epsilon 1}$)	2.18	3.08	2.99 ($N^{\eta 1}$)
	3.23 ($O^{\epsilon 2}$)			3.09 ($N^{\eta 2}$)
Zn-CPA/III	2.56 ($O^{\epsilon 1}$)	2.62	2.13	3.26 ($N^{\eta 1}$)
	2.50 ($O^{\epsilon 2}$)			
Zn-CPA/VI	2.48 ($O^{\epsilon 1}$)	2.20	2.62	3.02 ($N^{\eta 1}$)
	2.92 ($O^{\epsilon 2}$)			3.51 ($N^{\eta 2}$)

blocking group binds)[36] can explain the dramatic increase in inhibition from analogue I to IV (observed K_i's are in the order of 10^{-6} and 10^{-8} M, respectively)[60] on the basis of specific interactions. As discussed below, information gleaned about interactions outside the specificity pocket can often be exploited to make a drug more specific for one member of a class of enzymes. Thus, while many zinc exoproteinases may have similar specificity pockets and active sites, they will generally differ greatly in the regions outside the active site. These differences can be used to render a given inhibitor highly specific for one enzyme, while having little effect on other related enzymes, although the active sites of the given family may be very similar.

It should be noted here that studies similar to the work described above for CPA were carried out in order to clarify the mechanism of action of aspartic proteinases. Series of inhibitors were designed to structurally mimic the tetrahedral intermediate encountered during the catalytic reaction, and these were examined when bound to penicillopepsin,[61,62] endothiapepsin,[63-65] and rhizopuspepsin.[66,67] The crystal structures of the complexes formed between penicillopespsin and the family of phosphorus-containing peptide analogues, where the scissile peptide bond (–CONH–) was replaced with a –$POOHCH_2$– group, were solved,[61] as well as the complexes with difluorinated analogues of statin and statone.[62] These studies revealed important details related to the enzyme interactions with a transition state. For example, the crystal structures of the enzyme/inhibitor structures of penicillopepsin showed intimate interactions for the stabilization of a *gem* diol intermediate via strong hydrogen bonds to the carboxyl groups of Asp33 and Asp213 of the active site. Endothiapepsin has been complexed with statin, some hydroxyethylene (–$CHOHCH_2$–) transition-state analogues and difluorostatone, and was found to form analogous short hydrogen bonds in the active site.[63-65] The structures reported for complexes of endothiapepsin indicate that the two aspartic groups in the active site, Asp215 and Asp32, stabilize the transition state by short hydrogen bonds, in a fashion similar to those observed in penicillopepsin. Similar studies were done with rhizopuspepsin and a series of inhibitors, and the structures obtained fully supported the mechanism in which the dihydroxy intermediate is stabilized by strong hydrogen bonds from Asp35 and Asp218 of the active site.[66,67]

Ketomethylene substrate analogues have also been shown to inhibit such enzymes as leucine–aminopeptidase and arginyl–aminopeptidase,[68] where similar short intermolecular hydrogen bonds have been shown to play an important role in the active site binding and in the actual catalysis. In correlation with the studies discussed above, these kinetic studies also suggest the stabilization of a intermediate *gem* diolate which is "trapped" in the enzyme active site. The variety of representative examples shown above suggest, therefore, that a *gem* diolate intermediate may be a rather common species in enzymatic proteolytic reactions, and that multiple strong hydrogen bonds of this *gem* diolate to active site functional groups may be a common enzymatic means by which these intermediates and the transition states associated with them are stabilized.

MECHANISTIC CONCLUSIONS

The combined results of the structural studies of the CPA complexes described above may be used to clarify some of the unresolved mechanistic questions discussed earlier. Although the benzyl succinate inhibitor and the ketomethylene pseudopeptides are quite different structures, it is interesting to note the similarity in their interactions with the zinc ion and two other residues. Both of them bind to the zinc as bidentate ligands, replacing the zinc-bound water, and both of them form strong hydrogen bonds with Arg127 and Glu270. A superposition of the zinc environment of the native-CPA complexes of BS and analogue I is shown in Figure 13, where it is demonstrated that the A-carboxylate group of BS and the *gem* diolate of I occupy an almost identical position in the active site. The tight binding of the two affectors is not surprising assuming that both structures resemble the tetrahedral intermediate in much the same way as the phosphonate analogues which exhibit even tighter binding.[31,69,70]

These results indirectly lend some support to the combined mechanism discussed above and clarify some of the roles that various active site residues play in catalysis and inhibition. The zinc ion appears to influence binding of substrates; the presence of compensating charges on other residues in the

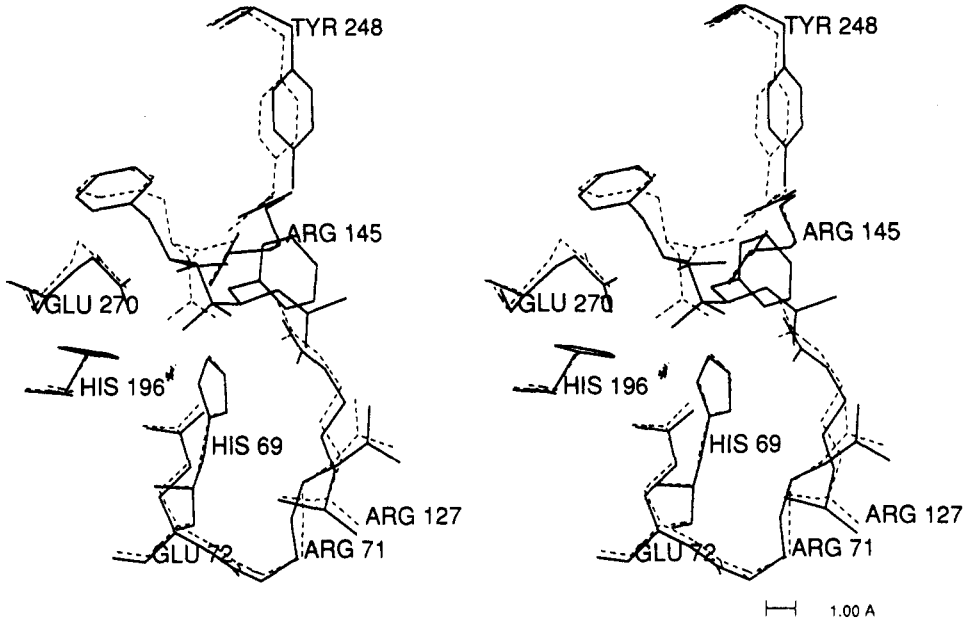

Figure 13. Stereoview comparison of the active site of CPA complexed with acetyl-Phe-Ψ-Phe (thick lines) and the active site complexed with benzyl succinate (dashed lines).

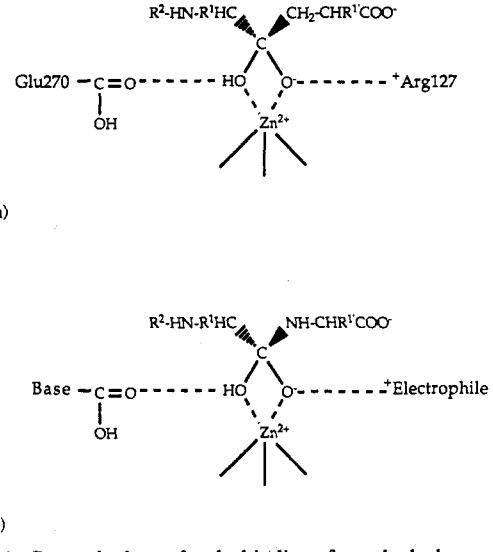

Figure 14. General scheme for the binding of tetrahedral *gem* diolates in the active site of zinc proteinases: (a) binding observed with hydrated ketomethylene pseudopeptides in the active site of CPA; (b) the possible binding of a tetrahedral transition state (intermediate) during cleavage of a peptide substrate corresponding to the structure seen in a.

active site seems to be insufficient to effectively bind substrates or inhibitors if the zinc ion is removed. The zinc also stabilizes transition states along the reaction pathway, in addition to its proposed roles in the actual chemistry of the reaction. Arg127 and Glu270, and to some extent Arg145, appear to play a role in stabilizing the transition states that evolve during the course of the reaction, as deduced by the interactions these residues make with the bound inhibitors. Since residues of similar characteristics and geometry are present in other zinc proteinases, these roles are likely to be general for the mode of action of this family. Hence, the negatively charged tetrahedral intermediate of the general hydrolytic reaction is neutralized and stabilized by a combination of interactions with the zinc ion, the base, and the electrophile of the catalytic tetrad, as outlined schematically in Figure 14. Possible roles in forming the Michaelis–Menten complex require further investigation.

CONSIDERATIONS OF SURFACE INTERACTIONS

While the most common graphical representation of proteins is by line vectors between point atoms, this does not reproduce the "surface" of the molecule created by the exclusive nature of the van der Waals radii of the atoms. In contrast, hard-sphere (CPK) models of molecules map out the detailed molecular surface according to the radii of the atoms.[71] The surface thus viewed gives a general idea of how the molecule is "seen" by other molecules which encounter it, at least in terms of van der Waals' forces, which are surface contact effects. The hard-surface representation, however, does not account for the size or shape of the other contacting molecule. Thus "crevices" or "valleys" created between the spheres on a van der Waals' surface may not be accessible to all solvent molecules depending on the size of the solvent in question. Even reasonably large holes in the surface of a protein may not be large enough to allow entry of all solvent molecules. Thus, a different type of surface should be calculated for studying the practical surface of a given molecule. One possible representation is referred to as the "solvent accessible surface". The method used to generate the surface uses a sphere of a given radius to approximate the desired solvent molecule, and rolls this sphere around the van der Waals' surface of the protein. The surface of contact between the edge of the sphere and the surface of the protein is then referred to as the *solvent accessible surface*.[72] The surface generated in this fashion excludes holes or gaps in the protein which are too small to allow entry of the solvent molecule in question.

The utility of these surfaces can be demonstrated by the following example. The strong binding of substrates to enzymes has a significant contribution from the van der Waals' forces acting between the contacting surfaces of the two molecules. The greater the complementarity between the two surfaces, the greater the contribution to binding energy. Comparison of the solvent accessible surface of the active site of the enzyme with that of the substrate could be used, therefore, to gauge the extent of the complementarity between the two molecules and hence to evaluate the relative binding energetics. In a simplistic model, adjustments to the substrate which fill empty areas between the two surfaces should increase the binding strength of the substrate, as long as the added

Figure 15. Solvent accessible surface plot (stereoview) of CPA with a proposed model for the binding of the inhibitor benzoyl-Phe-Phe-Ψ-Phe (VII). The dot surface represents the solvent accessible surface of CPA without the inhibitor, calculated using the conformation of CPA found in the complex with acetyl-Phe-Ψ-Phe. The radius of the probe used for the surface calculation was 1.7 Å. The electron density wire cage enclosing the inhibitor was contoured at the van der Waals' radius of its atoms. Note that this "surface" (also known as a Barry surface) is less extensive than the solvent accessible surface and so does not complement the surface of the enzyme as well. This type of surface was chosen only due to limitations in displaying the highly complementary solvent accessible interface between two surfaces in black and white.

groups do not penetrate into the surface of the protein to a significant degree. Thus one can "tailor" a given substrate or inhibitor to better match the protein surface presented, and so increase the binding constant.

Several caveats must be considered when employing this method, some of which are outlined below. Firstly, the enzyme may change its shape when a substrate binds. Thus, surfaces calculated using the native enzyme may not show available cavities which would be formed by conformational changes effected by substrate binding. Even if one were to use a structure of an enzyme with a bound inhibitor as the basis for the calculation, one cannot be certain that any observed high complementarity may not be due to the enzyme adapting itself to the shape of the bound molecule in an optimal way.

Secondly, this method does not account for charge–charge interactions, which could greatly influence binding energy, either favorably or disfavorably.

In addition to these considerations, it should be noted that the generated surface is sensitive to the radius of the probe used, and thus changes of this parameter would influence the results.

As discussed above, a series of ketomethylene inhibitors has been prepared, with varying moieties placed on the N-terminus side of the inhibitor. Kinetic studies have shown variations in the inhibition constants which are caused by changes in the N-terminal blocking moiety.[60] It should be possible to use the surface calculations discussed here to provide some basis for the differing affinities observed for the various analogue derivatives by examining how well the N-terminal side of the molecule interacts with the surface of the protein outside the active site. Toward this end, a study is being initiated which examines the relationship between the surface area of contact between the N-terminal blocking group and the enzyme. This region is important for drug design, since it represents the unique binding region of the enzyme under study. Thus, in this example, it may be that enzymes which perform the same function as CPA, which is cleaving off a hydrophobic C-terminus residue, will likely have very similar binding pockets. The differences in binding specificity, then, will lie in the extended binding regions, outside the active site pocket. The goal of this type of study is to identify which aspects of the extended binding region allow an inhibitor to bind tightly to a given enzyme, but not to other enzymes of similar function.

Initial analysis indicates that there is a high degree of complementarity in the active site pocket between the enzyme and the inhibitors. There is some room between the C-terminal phenyl side chain and the surface of the enzyme, indicating that there might be room for another substituent, such as $-CH_3$, in the *para* position of the phenyl ring. This could lead to an improvement in the hydrophobic contact area, and so increase the binding constant. This, of course, requires confirmation by actual synthesis and testing.

A close complementarity is also observed between the penultimate side chain and the enzyme surface, demonstrating the known specificity at this site.[29]

Of greater interest are the interactions beyond the active site, in the open binding cleft on the surface of the enzyme, as mentioned above. This region is a long, fairly hydrophobic depression, which in part explains the increase in binding constant seen for the larger N-terminal blocking groups in the ketomethylene series.[60] An example of this is shown in Figure 15 where some aspects of the proposed surface interactions of CPA and ketomethylene analogue benzoyl-Phe-Phe-Ψ-Phe (VII) are examined. The model for this interaction was based upon the known structures of the complexes between CPA and analogues I and IV. Kinetic measurements show that this is the most tightly binding ketomethylene studied to date, in keeping with the hypothesis that increasing the hydrophobic nature of the extended inhibitor will increase binding affinity. Exact guidelines as to which inhibitor substituents would best interact in the extended binding site require more extensive examples of enzyme/inhibitor complexes and more exacting mathematical treatment. Nevertheless, these preliminary and simplistic studies do give general guidelines as to which major factors might affect inhibitor affinity.

CONSIDERATIONS OF ELECTROSTATIC POTENTIALS

In order to evaluate the contribution of long range electrostatic interactions in the mode of action of the enzyme, the algorithm DelPhi was used, which calculates electrostatic potentials of molecules, based on their three dimensional distribution of charged atoms.[73,74]

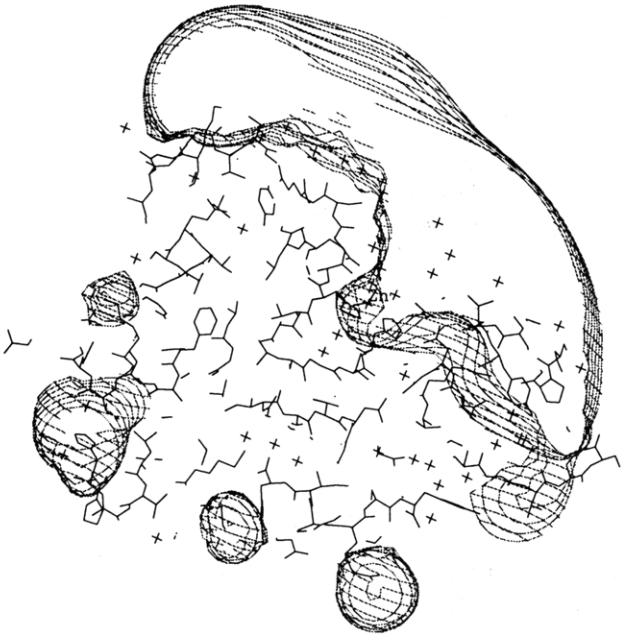

Figure 16. Electrostatic potential contours for CPA, calculated using the program DelPhi. The contour level is 1.0 kT/e, showing quite a large region of positive electrostatic potential emanating from the active site at physiological pH. (The active site Zn is shown, center.)

Specifically, the program was used to examine the electrostatic potential around the active site of CPA. Since the enzyme must bind the negatively charged C-terminus of a substrate, we used DelPhi to investigate what role electrostatics might play in attracting the molecule to the active site, and to what extent, if any, the metal might contribute to this effect.

The calculation was performed on native-CPA, in a medium of water, at physiological pH and ionic strength. The result (Figure 16) showed a prominent concentration of positive electrostatic potential emanating from the active site. In an attempt to estimate the contribution of the zinc ion to the observed potential, the calculation was repeated with the zinc removed (apo-CPA). A great reduction in the positive potential around the active site was observed; in fact, negative electrostatic potential emanates from the active site, as shown in Figure 17. In the apo-enzyme, however, there is a salt bridge formed between the side chains of His196 and Glu270, as discussed above. This implies that His196 side chain bears a full positive charge. His69 would also likely bear a full positive charge in the absence of zinc, since its $N^{\epsilon 2}$ lies within 2.9 Å of Asp142$O^{\delta 1}$, and its $N^{\delta 1}$ is 3.1 Å away from Glu72$O^{\epsilon 1}$. If the calculation is repeated with a full charge on His196 and His69, the long range distribution of electrostatic potentials resembles, at least partially, the potentials obtained for the native enzyme. Thus any long range electrostatic contribution to substrate binding arising from the metal ion in the active site could be compensated for by protonation of the two ion-coordinating residues in the apo-enzyme. The apparent inability to bind substrate in the active site of apo-CPA in the soaking experiments described above indicates that close range electrostatic effects of the zinc ion are important in binding substrates and inhibitors.

Other uses of DelPhi include the calculation of the change in pH of a certain group in going from one environment (e.g. completely exposed in solution) to another environment (e.g. partially buried in an active site). This can give clues as to the expected protonation states of various residues in the active site of an enzyme, since the removal from water can often be offset by interaction with other charged or partially charged groups.

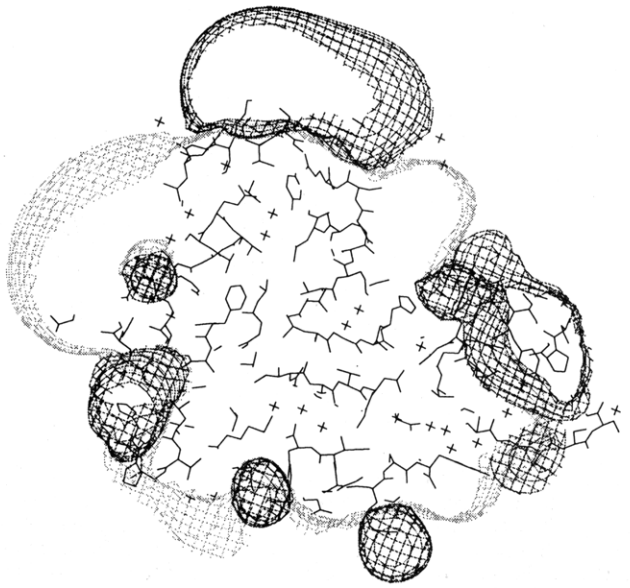

Figure 17. Electrostatic potential contours for apo-CPA, where no compensating charges have been placed on Histidines 69 and 196. The dark contours are at +1.0 kT/e, while the lighter contours are at −1.0 kT/e. This clearly shows that the positive electrostatic potential emanating from the active site of native-CPA is gone, and has been replaced by a negative potential. (Orientation of CPA here is identical to that in Figure 16.) If both His69 and His196 are given positive charges, a potential map similar to native-CPA is obtained.

It must be remembered, however, that the accuracy of results obtained from this program is not likely to be good enough to make absolute statements about electrostatic energies. Rather, trends can be observed, and significance can be placed on relative changes in potentials.

SUMMARY

This work has reviewed some of the ways in which recent advancements in computer technologies are exploited in the field of protein research and in particular, X-ray crystallography. Faster computers and graphics sub-systems have greatly enriched the tools available to crystallographers and have greatly decreased the time required for many stages in the course of structure solution.

Specifically, the studies presented here into the mechanism of action of CPA have been greatly enhanced by the powerful hardware and software currently available to researchers. What has emerged from these studies is as follows.

Removal of the active site zinc ion from CPA results in only minor structural changes. Furthermore, the apo-enzyme does not appear capable of binding peptide substrates, in a any significant way relative to the native enzyme. This suggests that the zinc plays a role in the binding of peptide substrates in the active site. Although long range electrostatic attraction may play a role in substrate/inhibitor binding, these forces appear incapable of causing a substrate to remain bound in the active site in the absence of zinc. In addition to its proposed direct participation in the catalytic process, the zinc ion also appears to stabilize at least one of the transition states or intermediates that is formed during substrate hydrolysis.

The inhibitor benzyl succinate resembles a tetrahedral intermediate in its mode of binding. Replacement of the metal in the active site of CPA does not appear to alter the binding mode of this inhibitor, suggesting that changes in activity observed upon metal replacement are not caused by changes in substrate binding. This points to differences in electronic properties as being the source for the observed changes in

activity. Artifacts arising from solvent–metal interactions may also be responsible for some of the activity changes.

The ketomethylene inhibitor studies strongly implicate the zinc-bound water as the attacking nucleophile and show that the active site base and electrophile (Glu270 and Arg127) act at least to stabilize the tetrahedral intermediate.

While these studies do not provide a complete picture of the catalytic process carried out by CPA, they do provide information about certain stages along the reaction coordinate. Furthermore, this information should be applicable to related zinc exo-proteinases, and possibly even to other zinc proteinases in general.

ACKNOWLEDGMENT

We are indebted to P. Tucker for the important technical assistance with the crystallographic data measurement of several of the CPA derivatives. We acknowledge the extensive work done by C. Gilon and V. Rashti in the synthesis and kinetic characterization of the ketomethylene analogues. We thank O. Almog for various technical assistance and fruitful discussions, and the Unit of Interdepartmental Services of the Institute of Life Sciences for providing us with some of the equipment needed for biochemical analysis. We acknowledge the comments of one of the manuscript reviewers which drew our attention to recent relevant studies of inhibitors with aspartyl proteases. We thank the Israeli Academy of Sciences (Grant No. 253/88), the Friends of the Hebrew University in England, Ms. Myrtle Franklin, and the Bat Sheva de Rothchild Foundation for financial support. H.F. thanks the Wolf Foundation for predoctoral fellowship.

REFERENCES AND NOTES

(1) Vallee, B. L.; Galdes, A.; Auld, D. S.; Riordan, J. F. Carboxypeptidase A. In *Metal Ions in Biology*; Spiro, T.G., Ed.; Wiley: New York, 1983; Vol. 5, pp 25–75.

(2) Vallee, B. L.; Galdes, A. The metallobiochemistry of zinc enzymes. *Adv. Enzymol.* **1984**, *56*, 283–430.

(3) Vallee, B. L. A synopsis of zinc biology and pathology. *Zinc Enzymes*; Birkhauser: Boston, 1986; PBB Vol. 1, pp 1–15.

(4) Rees, D. C.; Lewis, M.; Lipscomb, W. N. Refined crystal structure of carboxypeptidase A at 1.54 Å resolution. *J. Mol. Biol.* **1983**, *168*, 367–387.

(5) Schmid, M. F.; Herriott, J. R. Structure of carboxypeptidase B at 2.8 Å resolution. *J. Mol. Biol.* **1976**, *103*, 175–190.

(6) Holmes, M. A.; Matthews, B. W. Structure of thermolysin refined at 1.6 Å resolution. *J. Mol. Biol.* **1982**, *160*, 623–639.

(7) Dideberg, O.; Charlier, P.; Dive, G.; Joris, B.; Frere, J. M.; Ghuysen, J. M. Structure of a Zn^{2+}-containing D-alanyl-D-alanine-cleaving carboxypeptidase at 2.5 Å resolution. *Nature (London)* **1982**, *299*, 469–470.

(8) Pauptit, R. A.; Karlsson, R.; Picot, D.; Jenkins, J. A.; Niklaus-Reimer, A. S.; Jansonius, J. N. Crystal structure of neutral protease from *Bacillus cereus* refined at 3.0 Å resolution and comparison with the homologous but more thermostable enzyme thermolysin. *J. Mol. Biol.* **1988**, *199*, 525–537.

(9) Kester, W. R.; Matthews, B. W. Comparison of the structures of carboxypeptidase A and thermolysin. *J. Biol. Chem.* **1977**, *252*, 7704–7710.

(10) Argos, P.; Garavito, R. M.; Eventoff, W.; Rossmann, M. G. Similarities in active center geometries of zinc-containing enzymes. *J. Mol. Biol.* **1978**, *126*, 141–158.

(11) Christianson, D. W.; Lipscomb, W. N. Comparison of carboxypeptidase A and thermolysin inhibition by phosphonamidates. *J. Am. Chem. Soc.* **1988**, *110*, 5560–5565.

(12) Matthews, B. W. Structural basis of the action of thermolysin and related zinc peptidases. *Acc. Chem. Res.* **1988**, *21*, 333–340.

(13) Lipscomb, W. N. Carboxypeptidase A mechanisms. *Proc. Natl. Acad. Sci. U.S.A.* **1980**, *77*, 3875–3878.

(14) Christianson, D. W.; Lipscomb, W. N. Carboxypeptidase A. *Acc. Chem. Res.* **1989**, *22*, 62–69.

(15) (a) Soffer, R. L. Angiotensin-converting enzyme and the regulation of vasoactive peptides. *Annu. Rev. Biochem.* **1976**, *45*, 73–94. (b) Ondetti, M. A.; Cushman, D. W. Enzymes of the renin-angiotensin system and their inhibitors. *Ibid.* **1982**, *51*, 283–308.

(16) (a) Malfroy, B.; Swerts, J. P.; Guyon, A.; Roques, B. P.; Schwartz, J. C. High-affinity enkephalin-degrading peptidase in brain is increased after morphine. *Nature* **1978**, *276*, 523–526. (b) Schwartz, J. C.; Gros, C.; Lecomte, J. M.; Bralet, J. Enkephalinase (EC 3.4.24.11) inhibitors: protection of endogenous ANF against inactivation and potential therapeutic applications. *Life Sci.* **1990**, *47*, 1279–1297.

(17) (a) Waldschmidt-Leitz, E.; Purr, A. *Ber. Deut. Chem. Ges.* **1929**, *62*, 2217–2226. (b) Anson, M. L. Crystalline carboxypolypeptidase. *Science* **1935**, *81*, 467–468.

(18) Vallee, B. L.; Rupley, J. A.; Coombs, T. L.; Neurath, H. The release of zinc from carboxypeptidase and its replacement. *J. Am. Chem. Soc.* **1958**, *80*, 4750–4751.

(19) (a) Coleman, J. E.; Vallee, B. L. Metallocarboxypeptidases. *J. Biol. Chem.* **1960**, *235*, 390–395. (b) Coleman, J. E., Vallee, B. L. Metallocarboxypeptidases: Stability constants and enzymatic characteristics. *J. Biol. Chem.* **1961**, *236*, 2244–2249.

(20) Neurath, H.; Bradshaw, R. A.; Petra, P. H.; Walsh, K. A. Carboxypeptidase. Bovine carboxypeptidase A-activation, chemical structure and molecular heterogeneity. *Philos. Trans. R. Soc. London, Ser. B* **1970**, *257*, 159–176.

(21) Lipscomb, W. N.; Hartsuck, J. A.; Reeke, G. J.; Quiocho, F. A.; Bethge, P. H.; Ludwig, M. L.; Steitz, T. A.; Muirhead, H.; Coppola, J. C. The structure of carboxypeptidase A. The 2.0 Å resolution studies of the enzyme and its complex with glycyltyrosine, and mechanistic deductions. *Brookhaven Symp. Biol.* **1968**, *21*, 24–90.

(22) (a) Quiocho, F. A.; Richards, F. M. The enzymic behavior of carboxypeptidase A in the solid state. *Biochemistry* **1966**, *5*, 4062–4076. (b) Quiocho, F. A.; McMurray, C. H.; Lipscomb, W. N. Similarities between the conformation of arsanilazotyrosine 248 of carboxypeptidase A in the crystalline state and in solution. *Proc. Natl. Acad. Sci. U.S.A.* **1972**, *69*, 2850–2854.

(23) Rees, D. C.; Lipscomb, W. N. Refined crystal structure of the potato inhibitor complex of carboxypeptidase A at 2.5 Å resolution. *J. Mol. Biol.* **1982**, *160*, 475–498.

(24) Rees, D. C.; Lipscomb, W. N. Crystallographic studies on apocarboxypeptidase A and the complex with glycyl-L-tyrosine. *Proc. Natl. Acad. Sci. U.S.A.* **1983**, *80*, 7151–7154.

(25) Christianson, D. W.; Lipscomb, W. N. Binding of possible transition state analogue to the active site of carboxypeptidase A. *Proc. Natl. Acad. Sci. U.S.A.* **1985**, *82*, 6840–6844.

(26) Christianson, D. W.; Lipscomb, W. N. Novel structure of the complex between carboxypeptidase A and ketonic structure analogue. *J. Am. Chem. Soc.* **1985**, *107*, 8281–8283.

(27) (a) Christianson, D. W.; Lipscomb, W. N. Structure of the complex between an unexceptedly hydrolyzed phosphonamidate inhibitor and carboxypeptidase A. *J. Am. Chem. Soc.* **1986**, *108*, 545–546. (b) Christianson, D. W.; Lipscomb, W. N. The complex between carboxypeptidase A and possible transition state analogue: mechanistic inferences from high-resolution X-ray structures of enzyme-inhibitor complexes. *J. Am. Chem. Soc.* **1986**, *108*, 4998–5003. (c) Christianson, D. W.; Lipscomb, W. N. Carboxypeptidase A: novel enzyme-substrate-product complexes. *J. Am. Chem. Soc.* **1987**, *109*, 5536–5538.

(28) Christianson, D. W.; David, P. R.; Lipscomb, W. N. Mechanism of carboxypeptidase A: hydration of a ketonic substrate analogue. *Proc. Natl. Acad. Sci. U.S.A.* **1987**, *84*, 1512–1515.

(29) Shoham, G.; Christianson, D. W.; Oren, D. A. Complex between carboxypeptidase A and a hydrated ketomethylene substrate analogue. *Proc. Natl. Acad. Sci. U.S.A.* **1988**, *85*, 684–688.

(30) Christianson, D. W.; Mangani, S.; Lipscomb, W. N.; Shoham, G. Binding of D-phenylalanine and D-tyrosine to carboxypeptidase A. *J. Biol. Chem.* **1989**, *264*, 12849–12853.

(31) Kim, H.; Lipscomb, W. N. Comparison of the structure of three carboxypeptidase A–Phosphonate complexes determined by X-ray crystallography. *Biochemistry* **1991**, *30*, 8171–8180.

(32) Mangani, S.; Carloni, P.; Orioli, P. Crystal Structure of the Complex between Carboxypeptidase A and the Biproduct Analog Inhibitor L-Benzylsuccinate at 2.0 Å Resolution. *J. Mol. Biol.* **1992**, *223*, 573–578.

(33) Mangani, S.; Carloni, P.; Orioli, P. X-ray diffraction study of the interaction between carboxypeptidase A and (S)-(+)-1-amino-2-phenylethyl phosphonic acid. *Eur. J. Biochem.* **1992**, *203*, 173–177.

(34) Mangani, S.; Orioli, P. Crystal Structure of the Ternary Complex between Carboxypeptidase A, L-Phenylalanine, and Azide Ion. *Inorg. Chem.* **1992**, *31*, 365–368.

(35) Shoham, G.; Rees, D. C.; Lipscomb, W. N. Effects of pH on the structure and function of carboxypeptidase A: crystallographic studies. *Proc. Natl. Acad. Sci. U.S.A.* **1984**, *81*, 7767–7771.

(36) Abramowitz, N.; Schechter, I.; Berger, A. On the size of the active site in proteases. *Biochem. Biophys. Res. Commun.* **1967**, *29*, 862–867.

(37) Lipscomb, W. N. Acceleration of reactions by enzymes. *Acc. Chem. Res.* **1982**, *15*, 232–238.

(38) (a) Mock, W. L. Torsional Strain Considerations in the Mechanism of the Proteolytic Enzymes, with Particular Application to Carboxypeptidase A. *Bioorg. Chem.* **1975**, *4*, 270–278. (b) Mock, W. L.; Chen, J. T. The pH dependence of peptide hydrolysis by nitrocarboxypeptidase A. *Arch. Biochem. Biophys.* **1980**, *203*, 542–552.

(39) Lipscomb, W. N. Structure and catalysis of enzymes. *Annu. Rev. Biochem.* **1983**, *52*, 17–34.

(40) Monzingo, A. F.; Matthews, B. W. Binding of *N*-carboxymethyl dipeptide inhibitors to thermolysin determined by X-ray crystallography: A novel class of transition state analogues for zinc peptidases. *Biochemistry* **1984**, *23*, 5724–5729.
(41) Hangauer, D. G.; Monzingo, A. F.; Matthews, B. W. An interactive computer graphics study of thermolysin-catalyzed peptide cleavage and inhibition by *N*-carboxymethyl dipeptides. *Biochemistry* **1984**, *23*, 5730–5741.
(42) Shibata, A. Diffraction Data Collection with R-Axis-II, an X-ray Detecting System Using Imaging Plate. *Rigaku J.* **1990**, *7*, 28–32.
(43) Sato, M.; Yamamoto, M.; Imada, K.; Katsube, Y.; Tanaka, N.; Higashi, T. A High-Speed Data-Collection System for Large-Unit-Cell Crystals using an Imaging Plate as a Detector. *J. Appl. Crystallogr.* **1992**, *25*, 348–357.
(44) Krause, K. L.; Phillips, G. N. Experience with Commercial Area Detectors: A 'Buyers' Prespective. *J. Appl. Crystallogr.* **1992**, *25*, 146–154.
(45) Hendrickson, W. A.; Konnert, J. In *Biomolecular Structure, Function, Conformation and Evolution*; Srinivasan, R., Ed.; Pergamon Press: Oxford, U.K., 1981; Vol. 1, pp 43–47.
(46) Brünger, A. T. X-PLOR, Version 2.1, Yale University, New Haven, CT, 1990.
(47) Luzzati, V. *Acta Crystallogr.* **1952**, *5*, 802–810.
(48) Shoham, G.; Nechushtai, R.; Steppun, J.; Nelson, H.; Nelson, N. Unpublished results.
(49) (a) Maret, W. Methodology of Metal Exchange in Metalloproteins. In *Zinc Enzymes*; Birkhauser: Boston, 1986; PBB Vol. 1, pp 17–26. (b) Bertini, I.; Luchinat, C.; Viezzoli, M. S. Metal Substitution as a Tool for the Investigation of Zinc Proteins. In *Zinc Enzymes*; Birkhauser: Boston, 1986; PBB Vol. 1, pp 27–47.
(50) Hardman, K. D.; Lipscomb, W. N. Structures of nickel(II) and cobalt-(II) carboxypeptidase A. *J. Am. Chem. Soc.* **1984**, *106*, 463–464.
(51) Rees, D. C.; Howard, J. B.; Chakrabarti, P.; Yeates, T.; Hsu, B. T.; Hardman, K. D.; Lipscomb, W. N. Crystal Structures of Metallosubstituted Carboxypeptidase A. In *Zinc Enzymes*; Birkhauser: Boston, 1986; PBB Vol. 1, pp 155–165.
(52) Byers, L. D.; Wolfenden, R. A potent reversible inhibitor of carboxypeptidase A. *J. Biol. Chem.* **1972**, *247*, 606–608.
(53) Byers, L. D.; Wolfenden, R. Binding of the biproduct analog benzylsuccinic acid by carboxypeptidase A. *Biochemistry* **1973**, *12*, 2070–2078.
(54) (a) Cushman, D. W.; Ceung, H. S.; Sabo, E. F.; Ondetti, M. A. Design of potent competitive inhibitors of Angiotensin-converting enzyme. Carboxyalkanoyl and mercaptoalkanoyl amino acids. *Biochemistry* **1977**, *16*, 5484–5491. (b) Patchett, A. A.; *et al.* A new class of Angiotensin converting enzyme inhibitor. *Nature* (*London*) **1980**, *288*, 280–283.
(55) Martin, M. T.; Holmquist, B.; Riordan, J. F. An Angiotensin Converting Enzyme Inhibitor is a Tight-binding Slow substrate of Carboxypeptidase A. *J. Inorg. Biochem.* **1989**, *36*, 27–37.
(56) Bicknell, R.; Schaffer, A.; Bertini, I.; Luchinat, C.; Vallee, B. L.; Auld, D. S. Interaction of anions with the active site of carboxypeptidase A. *Biochemistry* **1988**, *27*, 1050–1057.
(57) Bolognesi, M. C.; Matthews, B. W. Binding of the biproduct analog L-benzylsuccinic acid to thermolysin determined by X-ray crystallography. *J. Biol. Chem.* **1979**, *254*, 634–639.
(58) (a) Ewenson, A.; Cohen-Suissa, R.; Levian-Teitelbaum, D.; Selinger, Z.; Chorev, M.; Gilon, C. Synthesis of Keto-Methylene and dehydro-Keto-Methylene pseudo dipeptides. *Int. J. Peptide Protein Res.* **1988**, *31*, 269–280. (b) Ewenson, A.; Laufer, R.; Chorev, M.; Selinger, Z.; Gilon, C. Dehydro keto-methylene and keto-methylene analogues of substance P. *J. Med. Chem.* **1988**, *31*, 416–421.
(59) Shoham, G.; Oren, D. A.; Ewenson, A.; Gilon, C. Inhibition of Carboxypeptidase A with Keto-methylene Pseudopeptides. *Proceedings* of the *20th European Peptide Symposium*; de Gruyter: Berlin, 1988; pp 411–413.
(60) Rashti, V.; Feinberg, H.; Greenblatt, H.; Shoham, G.; Gilon, C. Unpublished results.
(61) Fraser, M. E.; Strynadka, N. C. J.; Barlett, P. A.; Hanson, J. E.; James, M. N. G. Crystallographic Analysis of Transition-State Mimics Bound to Penicillopepsin: Phosphorus-Containing Peptide Analogues. *Biochemistry* **1992**, *31*, 5201–5214.
(62) James, M. N. G.; Sielecki, A. R.; Hayakawa, K.; Gelb, M. H. Crystallographic Analysis of Transition-State Mimics Bound to Penicillopepsin: Difluorostatin- and Difluorostatone-Containing Peptides. *Biochemistry* **1992**, *31*, 3872–3886.
(63) Veerapandian, B.; Cooper, J. B.; Sali, A.; Blundell, T. L. X-ray Analyses of Aspartic Proteinases. III Three-dimensional Structure of Endothiapepsin Complexed with a Transition-state Isoster Inhibitor of Renin at 1.6 Å Resolution. *J. Mol. Biol.* **1990**, *216*, 1017–1029.
(64) Cooper, J. B.; Foundling, S. I.; Blundell, T. L.; Boger, J.; Jupp, R. A.; Kay, J. X-ray studies of aspartic proteinase–statine inhibitor complexes. *Biochemistry* **1989**, *28*, 8596–8603.
(65) Hoover, D. J.; Veerapandian, B.; Cooper, J. B.; Damon, D. B.; Dominy, B. W.; Rosati, R. L.; Blundell, T. L. X-ray analysis of difluorostatone renin inhibitor bound as the tetrahedral hydrate to aspartic protease endothiapepsin. *Adv. Exp.Med. Biol.* **1991**, *306*, 269–273.
(66) Parris, K. D.; Hoover, D. J.; Davies, D. R. Crystal Structures of *rhizopuspepsin*/inhibitor complexes. *Adv. Exp. Med. Biol.* **1991**, *306*, 217–231.
(67) Suguna, K.; Padlan, E. A.; Bott, R.; Boger, J.; Parris, K. D.; Davies, D. R. Structures of complexes of rhizopuspepsin with pepstatin and other statin-containing inhibitors. *Proteins* **1992**, *13* (3), 195–205.
(68) Harbeson, S. L.; Rich, D. H. Inhibition of Aminopeptidase by Peptides Containing Ketomethylene and Hydroxyethylene Amide Bond Replacements. *J. Med. Chem.* **1989**, *32*, 1378–1392.
(69) Hanson, J. E.; Kaplan, A. P.; Bartlett, P. A. Phosphonate Analogues of Carboxypeptidase A Substrates Are Potent Transition-State Analogue Inhibitors. *Biochemistry* **1989**, *28*, 6294–6305.
(70) Kaplan, A. P.; Bartlett, P. A. Synthesis and evaluation of an inhibitor of carboxypeptidase A with a *Ki* value in the femtomolar range. *Biochemistry* **1991**, *30*, 8165–8170.
(71) Richards, F. M. Areas, Volumes, Packing, and Protein Structure. *Annu. Rev. Biophys. Bioeng.* **1977**, *6*, 151–176.
(72) Connolly, M. L. Solvent-Accessible Surfaces of Proteins and Nucleic Acids. *Science* **1983**, *221*, 709–713.
(73) Gilson, M. K.; Honig, B. H. Calculations of Electrostatic Potentials in an Enzyme Active Site. *Nature* (*London*) **1987**, *330*, 84–86.
(74) Gilson, M. K.; Sharp, K. A.; Honig, B. H. Calculating the Electrostatic Potential of Molecules in Solution: Method and Error Assessment. *J. Comput. Chem.* **1988**, *9*, 327–335.